Journal of Applied and Computational Mechanics, Vol. 3, No. 3, (2017), 218-228
DOI: 10.22055/jacm.2017.21757.1115

Journal of
Applied and Computational Mechanics

Analytical predictions for the buckling of a nanoplate subjected to non-uniform compression based on the four-variable plate theory

Mohammad Malikan[1]

[1] Department of Mechanical Engineering, Faculty of Engineering, Islamic Azad University, Mashhad, Iran

Received April 15 2017; Revised May 05 2017; Accepted for publication May 08 2017.
Corresponding author: Mohammad Malikan, mohammad.malikan@yahoo.com

Abstract

In the present study, the buckling analysis of the rectangular nanoplate under biaxial non-uniform compression using the modified couple stress continuum theory with various boundary conditions has been considered. The simplified first order shear deformation theory (S-FSDT) has been employed and the governing differential equations have been obtained using the Hamilton's principle. An analytical approach has been applied to obtain exact results from various boundary conditions. Due to the fact that there is not any research about the buckling of nanoplates based on the S-FSDT including the couple stress effect, the obtained results have been compared with the molecular dynamic simulation and FSDT papers which use the Eringen nonlocal elasticity theory. At the end, the results have been presented by making changes in some parameters such as the aspect ratio, the effect of various non-uniform loads and the length scale parameter.

Keywords: Nonuniform compression; Modified couple stress theory; S-FSDT

1. Introduction

Graphene is a thin layer of pure carbon which contains a tightly packed layer of carbon atoms that are bonded together in a hexagonal honeycomb lattice [1]. Due to the ultrahigh strength of the graphene, its inclusions are effectively used in the enhancement of both strength and fracture toughness in composite materials [2]. For instance, in order to improve the fracture toughness of ceramic materials, several research groups fabricated nano composites consisting of ceramic matrixes and inclusions in the form of graphene platelets [2, 3]. Moreover, inclusions in the form of graphene sheets provide the enhancement of mechanical characteristics in the polymer-based nano composites [4]. For instance, partially oxygenated graphene sheets were dispersed in the polymer matrix, and mechanical characteristics of the resultant nano composites with various graphene contents were examined [5].

In the last several years, many research papers about mechanical behavior of graphene sheets have been presented [6-20]. Malekzadeh et al. [8] considered small scale effect on the thermal buckling of orthotropic arbitrary straight-sided quadrilateral nanoplates embedded in an elastic medium via the classical plate theory. Zenkour and Sobhy [9] analyzed the thermal buckling of a rectangular nano graphene sheet based on the Winkler-Pasternak foundation. The sine function and the sinusoidal plate theory were used to derive the equations. Murmu et al. [10] conducted the buckling analysis of bi-layer nano graphene in the nonlocal theory under biaxial compression via an analytical solution using the classical plate theory with linear strains. Besides, it was demonstrated that the nonlocal critical load was always less than the local critical load. Wang et al. [11] investigated the thermal buckling of a nanoscale plate via classical and Mindlin plate theories and by using the simply supported boundary condition. Malekzadeh and Alibeygi [12] analyzed the thermal buckling of an orthotropic single layer graphene sheet by using the nonlinear elastic foundation. The classical theory and the differential quadrature method along with the Winkler elastic foundation which was modeled with the nonlinear spring were used. The above -mentioned method serves as a bench mark for future research. Mohammadi et al. [13] studied the shear buckling of an orthotropic rectangular single layer nanoplate in the thermal environment by the classical plate theory. They showed that the difference

between the shear buckling load calculated by isotropic and orthotropic plates decreases by increasing the nonlocal parameter. Radic et al. [14] published a study on the mechanical buckling of a multi-layer rectangular graphene sheet based on an elastic foundation and found that the nonlocal effect had great influence on higher buckling modes. The exact solution for vibrations and the biaxial buckling of a multi-layer graphene sheet based on the Winkler elastic foundation were investigated by Murmu et al. [15]. The presented equations utilized the classical plate theory and proved that the critical temperature and natural frequencies were further affected by reducing the Winkler coefficient in high modes. Anjomshoa et al. [16] derived mechanical buckling equations of multi-layers of a rectangular graphene sheet placed on an elastic foundation using the classical plate theory and the finite element numerical method. Radebe and Adali [17] studied the buckling of rectangular nanoplates with uncertain orthotropic material properties using the non-local theory. They considered the nanoplate as a non-local plate to take the small-size effects into account along with the small-scale parameter which was also taken to be uncertain. They studied the effect of the small scale on natural frequencies. A new analytical solution for the buckling and vibration analysis of functionally graded sandwich beams using a quasi-3D shear deformation theory was presented by Nguyen et al. [18]. Golmakani and Rezatalab [19] conducted a study on the biaxial buckling of a single layer graphene plate by considering the elastic foundation and the non-uniform mechanical load. The results showed that by neglecting the elastic foundation, when the small scale effects were reduced, the critical load also decreased. Jamali et al. [20] presented the uniaxial buckling analysis comparison of a nanoplate and a nanocomposite plate with the central square cut out by using the domain decomposition method. They showed that the existence of a hole in the plate causes defects in the system and weakens the buckling behavior. The dynamic buckling of embedded laminated nanocomposite plates based on the sinusoidal shear deformation theory was studied by Zarei et al. [21]. Malikan et al. [22] published the buckling of a double-layered nanoplate under shear and thermal loads based on the elastic matrix using the differential quadrature method. They showed that the effect of the type of the shear loading on the nonlocal results was more than local results. Moreover, in the thermal buckling analysis, the most important results included the boundary conditions which had more flexibility and by increasing the dimension's ratio, the results of the critical temperature were tightly close together in the nonlocal and local analysis.

The main aim of this study is to give a brief overview of new theoretical considering on nanosheets under the biaxial buckling. Regarding the first order shear deformation theory, we could not get the right value for the shear correction factor to consider the shear stress distribution in the thickness direction. Therefore, the simplified first order shear deformation theory (S-FSDT) that provides a welcome alternative to solve this problem has been investigated. In the following sections, the nonlinear strain of Von-Karman has been considered and also the material properties have been assumed as orthotropic. In addition, in order to study the length scale and due to presence of the variable nonlocal parameter, the modified couple stress effect has been employed because there is a difficulty with the Eringen nonlocal elasticity to consider nano materials behavior in deriving of governing equations while it is applied on the nonlocal stress resultants. Moreover, the exact solution has been used to solve the stability equations. Finally, the effects of different parameters such as changes in the length scale parameter, the aspect ratio and boundary effects of edges in various conditions under non-uniform in-plane loads have been demonstrated.

2. Formulation

A rectangular nanoplate with thickness *h*, the length *Lx*, and the width *Ly* is considered (Fig.1). Of the many shear deformable plate theories proposed over the years, the FSDT is fundamentally simpler to adopt for modelling the shear deformation behavior of plates. Nowadays, the FSDT is widely in use because of its simplicity. It is obvious that in the plate analysis, shear deformation effects are significant not only for thick plates but even for thin plates [23]. Since the classical plate theory (CPT) does not take shear effects into the account, many theories have evolved to address the deficiency. According to the FSDT, the following displacement field can be expressed as:

$$U(x,y,z) = u(x,y) + z\varphi(x,y) \tag{1a}$$

$$V(x,y,z) = v(x,y) + z\psi(x,y) \tag{1b}$$

$$W(x,y,z) = w(x,y) \tag{1c}$$

where u, v and w are displacement components along x, y and z directions, respectively. Moreover, φ and ψ are the rotational displacement along the y and x directions, respectively. In this theory, the shear stress in the thickness direction is a constant value which in fact is not true. In contrast, in the S-FSDT theory it is assumed that the transverse displacement (w) is divided into the bending component (w_b) and the shear component (w_s) [24] as follows:

$$w = w(bending) + w(shear) \tag{2}$$

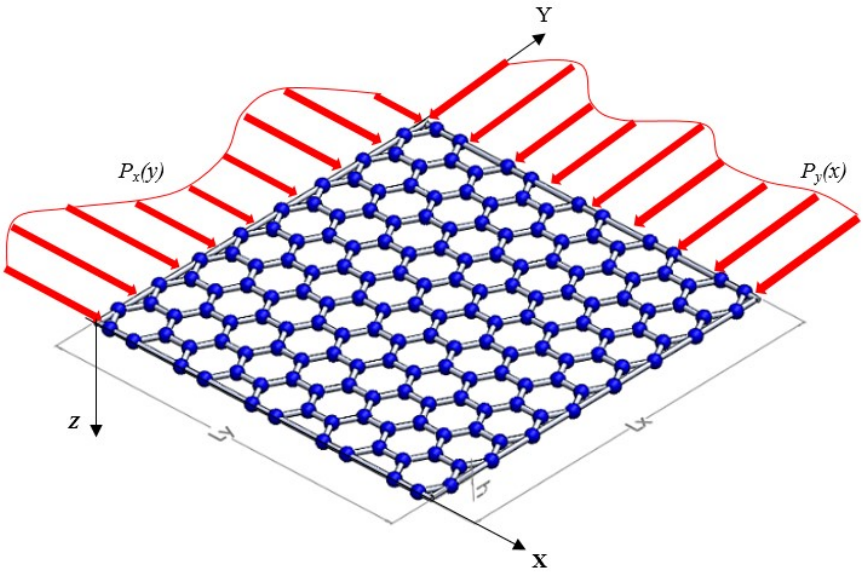

Fig.1. Schematic diagram of the rectangular nanoplate

Moreover, the rotation variable in the S-FSDT is expressed in terms of only the bending component as follows:

$$\varphi = -\frac{\partial w_b}{\partial x}$$
$$\psi = -\frac{\partial w_b}{\partial y} \tag{3}$$

By substituting Eqs. (2) and (3) into Eq. (1), the S-FSDT displacement field can be written as follows:

$$\begin{cases} U(x,y,z) = u(x,y) - z\dfrac{\partial w_b}{\partial x} \\ V(x,y,z) = v(x,y) - z\dfrac{\partial w_b}{\partial y} \\ W(x,y,z) = w_b(x,y) + w_s(x,y) \end{cases} \tag{4}$$

In recent years, various size dependent continuum theories such as the couple stress theory, the modified couple stress theory, the strain gradient theory and the nonlocal elasticity theory have been proposed. These theories are comprised of information about the inter-atomic forces and internal lengths. Among these theories, the nonlocal elasticity theory of Eringen has been widely applied. It should be noted that unique results cannot be found in this theory because the variable nonlocal parameter has to be used. The classical couple stress theory is one of the higher order continuum theories which contains two additional material length scale parameters along with the classical constants for an elastic material as elaborated by Mindlin and Tieresten [25], Toupin [26], and Koiter [27]. In fact, the couple stress theory is a special case of the micro-polar theory proposed by Cosserat brothers [28]. Recently, a modified couple stress theory, which contains only one additional material length scale parameter in addition to the classical material constants, was proposed by Yang et al. [29]. The modified couple stress theory is more useful than the classical one due to the symmetric couple stress tensor. According to this higher-order continuum theory and using the Hamilton's principle, the governing equations as well as the related boundary conditions along the edges of the rectangular nanoplate can be derived. The equations of the total potential energy (V) are expressed as follows:

$$V = U + \Omega \tag{5}$$

where U is the strain energy and Ω is the work done by external loads. The virtual strain energy can be calculated as follows:

$$\delta U = \iiint_v \left(\sigma_{ij}\delta\varepsilon_{ij} + m_{ij}\delta\chi_{ij}\right)dV = 0 \tag{6}$$

where σ_{ij}, ε_{ij}, m_{ij}, χ_{ij} are the stress tensor, the strain tensor, the deviatoric part of the couple stress tensor, and the symmetric curvature tensor, respectively [30-31].

$$\sigma_{ij} = \lambda\varepsilon_{kk}\delta_{ij} + 2\mu\varepsilon_{ij} \;;\quad \varepsilon_{ij} = \frac{1}{2}\left(\frac{\partial u_i}{\partial x_j} + \frac{\partial u_j}{\partial x_i} + \frac{\partial u_k}{\partial x_i}\frac{\partial u_k}{\partial x_j}\right),\ i,j,k=1,2,3 \tag{7}$$

$$m_{ij} = 2G_{xy}l^2\chi_{ij} \tag{8}$$

$$\chi_{ij}=\frac{1}{2}\left(\frac{\partial\theta_i}{\partial x_j}+\frac{\partial\theta_j}{\partial x_i}\right),\ i,j=1,2,3\ ;\ \theta_i=\frac{1}{2}e_{ijk}U_{k,j} \tag{9}$$

Where λ and μ are Lame constants, l is a material length scale parameter that is related to the size effect, and θ is the rotation vector. The tensors associated in the displacement field in Eqs. (7-9) are as follows:

$$\varepsilon_{xx}=\frac{\partial u}{\partial x}-z\frac{\partial^2 w_b}{\partial x^2}+\frac{1}{2}\left(\frac{\partial w_b}{\partial x}\right)^2+\frac{1}{2}\left(\frac{\partial w_s}{\partial x}\right)^2+\frac{\partial w_b}{\partial x}\frac{\partial w_s}{\partial x} \tag{10a}$$

$$\varepsilon_{yy}=\frac{\partial v}{\partial y}-z\frac{\partial^2 w_b}{\partial y^2}+\frac{1}{2}\left(\frac{\partial w_b}{\partial y}\right)^2+\frac{1}{2}\left(\frac{\partial w_s}{\partial y}\right)^2+\frac{\partial w_b}{\partial y}\frac{\partial w_s}{\partial y} \tag{10b}$$

$$\gamma_{yz}=\frac{\partial w_s}{\partial y} \tag{10c}$$

$$\gamma_{xz}=\frac{\partial w_s}{\partial x} \tag{10d}$$

$$\gamma_{xy}=\left(\frac{\partial u}{\partial y}+\frac{\partial v}{\partial x}\right)-2z\frac{\partial^2 w_b}{\partial x\,\partial y}+\left(\frac{\partial w_b}{\partial x}+\frac{\partial w_s}{\partial x}\right)\left(\frac{\partial w_b}{\partial y}+\frac{\partial w_s}{\partial y}\right) \tag{10e}$$

$$\begin{cases}\chi_x=\frac{1}{2}\left(2\frac{\partial^2 w_b}{\partial x\,\partial y}+\frac{\partial^2 w_s}{\partial x\,\partial y}\right)\\ \chi_y=\frac{1}{2}\left(-2\frac{\partial^2 w_b}{\partial x\,\partial y}-\frac{\partial^2 w_s}{\partial x\,\partial y}\right)\\ \chi_{xy}=\frac{1}{4}\left(-2\frac{\partial^2 w_b}{\partial x^2}+2\frac{\partial^2 w_b}{\partial y^2}-\frac{\partial^2 w_s}{\partial x^2}+\frac{\partial^2 w_s}{\partial y^2}\right)\\ \chi_{xz}=\frac{1}{4}\left(\frac{\partial^2 v}{\partial x^2}-\frac{\partial^2 u}{\partial x\,\partial y}\right)\\ \chi_{yz}=\frac{1}{4}\left(-\frac{\partial^2 u}{\partial y^2}+\frac{\partial^2 v}{\partial x\,\partial y}\right)\end{cases} \tag{11a-e}$$

By using the principle of minimum potential energy ($\delta V=0$), the nonlinear constitutive equations are derived as:

$$N_{x,x}+N_{xy,y}+\tfrac{1}{4}Y_{xz,xy}+\tfrac{1}{4}Y_{yz,yy}=0 \tag{12a}$$

$$N_{xy,x}+N_{y,y}-\tfrac{1}{4}Y_{xz,xx}-\tfrac{1}{4}Y_{yz,xy}=0 \tag{12b}$$

$$Q_{x,x}+Q_{y,y}+N_{xx}\left(\frac{\partial^2 w_s}{\partial x^2}+\frac{\partial^2 w_b}{\partial x^2}\right)+N_{yy}\left(\frac{\partial^2 w_s}{\partial y^2}+\frac{\partial^2 w_b}{\partial y^2}\right)+2N_{xy}\left(\frac{\partial^2 w_b}{\partial x\,\partial y}+\frac{\partial^2 w_s}{\partial x\,\partial y}\right)-Y_{xx,xy}+\tfrac{1}{2}Y_{yy,xy}+\tfrac{1}{4}Y_{xy,xx}-\tfrac{1}{4}Y_{xy,yy}=0 \tag{12c}$$

$$-M_{x,x}-2M_{xy,y}-M_{y,y}+N_{xx}\left(\frac{\partial^2 w_s}{\partial x^2}+\frac{\partial^2 w_b}{\partial x^2}\right)+N_{yy}\left(\frac{\partial^2 w_s}{\partial y^2}+\frac{\partial^2 w_b}{\partial y^2}\right)+2N_{xy}\left(\frac{\partial^2 w_b}{\partial x\,\partial y}+\frac{\partial^2 w_s}{\partial x\,\partial y}\right)-2Y_{xx,xy}+Y_{yy,xy}+\tfrac{1}{2}Y_{xy,xx}-\tfrac{1}{2}Y_{xy,yy}=0 \tag{12d}$$

Ni, *Mi* and *Qi (i= x, y, xy)* and *Yij (i= x, y, xy)* are the stress resultants and non-zero curvature resultants, respectively, as follows:

$$(N_x,N_y,N_{xy})=\int_{-h/2}^{h/2}(\sigma_x,\sigma_y,\sigma_{xy})dz \tag{13a}$$

$$(M_x,M_y,M_{xy})=\int_{-h/2}^{h/2}(\sigma_x,\sigma_y,\sigma_{xy})z\,dz \tag{13b}$$

$$(Q_x,Q_y)=\int_{-h/2}^{h/2}(\sigma_{xz},\sigma_{yz})dz \tag{13c}$$

$$\begin{Bmatrix} Y_{xx} \\ Y_{yy} \\ Y_{xy} \\ Y_{xz} \\ Y_{yz} \end{Bmatrix} = \int_{-h/2}^{h/2} \begin{Bmatrix} m_{xx} \\ m_{yy} \\ m_{xy} \\ m_{xz} \\ m_{yz} \end{Bmatrix} dz \tag{14}$$

The governing equations (Eq. 12) for the rectangular nanoplate can be rewritten as follows:

$$N_{\mathrm{x,x}} + N_{\mathrm{xy,y}} + \frac{1}{2}A_s\left(-\frac{\partial^4 u}{\partial x^2 \partial y^2} + \frac{\partial^4 v}{\partial x^3 \partial y}\right) + \frac{1}{2}A_s\left(-\frac{\partial^4 u}{\partial y^4} + \frac{\partial^4 v}{\partial x \partial y^3}\right) = 0 \tag{15a}$$

$$N_{\mathrm{xy,x}} + N_{\mathrm{y,y}} - \frac{1}{2}A_s\left(-\frac{\partial^4 u}{\partial x^3 \partial y} + \frac{\partial^4 v}{\partial x^4}\right) - \frac{1}{2}A_s\left(-\frac{\partial^4 u}{\partial x \partial y^3} + \frac{\partial^4 v}{\partial x^2 \partial y^2}\right) = 0 \tag{15b}$$

$$\begin{aligned} &Q_{\mathrm{x,x}} + Q_{\mathrm{y,y}} + N_{xx}\left(\frac{\partial^2 w_b}{\partial x^2} + \frac{\partial^2 w_s}{\partial x^2}\right) + N_{yy}\left(\frac{\partial^2 w_b}{\partial y^2} + \frac{\partial^2 w_s}{\partial y^2}\right) + 2N_{xy}\left(\frac{\partial^2 w_b}{\partial x \partial y} + \frac{\partial^2 w_s}{\partial x \partial y}\right) \\ &-\frac{1}{2}A_s\left(5\frac{\partial^4 w_b}{\partial x^2 \partial y^2} + 3\frac{\partial^4 w_s}{\partial x^2 \partial y^2}\right) - \frac{1}{4}A_s\left(\frac{\partial^4 w_b}{\partial x^4} + \frac{1}{2}\frac{\partial^4 w_s}{\partial x^4} + \frac{\partial^4 w_b}{\partial y^4} + \frac{1}{2}\frac{\partial^4 w_s}{\partial y^4}\right) = 0 \end{aligned} \tag{15c}$$

$$\begin{aligned} &-M_{x,x\,x} - 2M_{xy,x\,y} - M_{y,y\,y} + N_{xx}\left(\frac{\partial^2 w_b}{\partial x^2} + \frac{\partial^2 w_s}{\partial x^2}\right) + N_{yy}\left(\frac{\partial^2 w_b}{\partial y^2} + \frac{\partial^2 w_s}{\partial y^2}\right) + 2N_{xy}\left(\frac{\partial^2 w_b}{\partial x \partial y} + \frac{\partial^2 w_s}{\partial x \partial y}\right) \\ &-\frac{5}{2}A_s\left(2\frac{\partial^4 w_b}{\partial x^2 \partial y^2} + \frac{\partial^4 w_s}{\partial x^2 \partial y^2}\right) - \frac{1}{4}A_s\left(2\frac{\partial^4 w_b}{\partial x^4} + \frac{\partial^4 w_s}{\partial x^4} + 2\frac{\partial^4 w_b}{\partial y^4} + \frac{\partial^4 w_s}{\partial y^4}\right) = 0 \end{aligned} \tag{15d}$$

The axial and flexural rigidities of the orthotropic nanoplate are given as follows:

$$\left(A_{ij}, D_{ij}\right) = \int_{-\frac{h}{2}}^{\frac{h}{2}} \left(1, z^2\right) \mathrm{Q_{ij}} dz \quad (i,k = 1,2,6)$$

$$\begin{aligned} &Q_{11} = \frac{E_x}{1-\upsilon_{xy}\upsilon_{yx}},\ Q_{22} = \frac{E_y}{1-\upsilon_{xy}\upsilon_{yx}},\ Q_{12} = \frac{\upsilon_{yx}E_x}{1-\upsilon_{xy}\upsilon_{yx}},\ Q_{66} = G_{xy} \\ &Q_{11} = \frac{E}{1-\upsilon^2} = Q_{22},\ Q_{12} = \frac{\upsilon E}{1-\upsilon^2},\ Q_{66} = G \\ &H_{44} = H_{55} = Gh,\ C_{44} = C_{55} = G \end{aligned} \tag{16}$$

In Eq. (16), Aij, Bij and Dij are the extensional stiffness, the bending stiffness and the extension-bending coupling matrix, respectively. Moreover, Ex and Ey are the Young's elasticity modules, νxy and νyx are the Poisson's ratio and Gxy, Gxz and Gyz are the shear modules for orthotropic materials, respectively. The stress resultants in Eq. (13) in the displacement field by using Eq.16 are defined as follows:

$$\begin{bmatrix} N_{xx} \\ N_{yy} \\ N_{xy} \\ M_{xx} \\ M_{yy} \\ M_{xy} \\ Q_y \\ Q_x \end{bmatrix} = \begin{bmatrix} A_{11} & A_{12} & 0 & 0 & 0 & 0 & 0 & 0 \\ A_{12} & A_{22} & 0 & 0 & 0 & 0 & 0 & 0 \\ 0 & 0 & A_{66} & 0 & 0 & 0 & 0 & 0 \\ 0 & 0 & 0 & D_{11} & D_{12} & 0 & 0 & 0 \\ 0 & 0 & 0 & D_{12} & D_{22} & 0 & 0 & 0 \\ 0 & 0 & 0 & 0 & 0 & D_{66} & 0 & 0 \\ 0 & 0 & 0 & 0 & 0 & 0 & H_{44} & 0 \\ 0 & 0 & 0 & 0 & 0 & 0 & 0 & H_{55} \end{bmatrix} \times \begin{bmatrix} \frac{\partial u}{\partial x} + \frac{1}{2}\left(\frac{\partial w_b}{\partial x}\right)^2 + \frac{1}{2}\left(\frac{\partial w_s}{\partial x}\right)^2 + \frac{\partial w_b}{\partial x}\frac{\partial w_s}{\partial x} \\ \frac{\partial v}{\partial y} + \frac{1}{2}\left(\frac{\partial w_b}{\partial y}\right)^2 + \frac{1}{2}\left(\frac{\partial w_s}{\partial y}\right)^2 + \frac{\partial w_b}{\partial y}\frac{\partial w_s}{\partial y} \\ \frac{\partial u}{\partial y} + \frac{\partial v}{\partial x} + \left(\frac{\partial w_b}{\partial x} + \frac{\partial w_s}{\partial x}\right)\left(\frac{\partial w_b}{\partial y} + \frac{\partial w_s}{\partial y}\right) \\ -\frac{\partial^2 w_b}{\partial x^2} \\ -\frac{\partial^2 w_b}{\partial y^2} \\ -\frac{\partial^2 w_b}{\partial x \partial y} \\ \frac{\partial w_s}{\partial y} \\ \frac{\partial w_s}{\partial x} \end{bmatrix} \tag{17}$$

The non-uniform in-plane forces in pre-buckling conditions are as follows:

Parabolically varying in-plane load [32]:

$$\begin{cases} N_{xx} = -4k_1 N^0 \dfrac{y}{L_y}\left(1-\dfrac{y}{L_y}\right) \\ N_{yy} = -4k_2 N^0 \dfrac{x}{L_x}\left(1-\dfrac{x}{L_x}\right) \end{cases} \tag{18}$$

Sinusoidal varying in-plane load [33]:

$$\begin{cases} N_{xx} = -k_1 \dfrac{\pi}{2} N^0 \mathrm{Sin}\left(\dfrac{\pi y}{L_y}\right) \\ N_{yy} = -k_2 \dfrac{\pi}{2} N^0 \mathrm{Sin}\left(\dfrac{\pi x}{L_x}\right) \end{cases} \tag{19}$$

Linearly varying in-plane load [33-34]:

$$\begin{cases} N_{xx} = -k_1 N^0 \left(1-\eta \dfrac{y}{L_y}\right) \\ N_{yy} = -k_2 N^0 \left(1-\eta \dfrac{x}{L_x}\right) \end{cases} \tag{20}$$

Where in the above-mentioned linear load, $\eta=0$ (the uniform load), $\eta=1$ (the triangular load). Moreover, N^0 is the critical in-plane load in buckling conditions. By inserting Eqs. (17) and (18-20) in Eq. (15), and also by considering the pre-buckling condition, the stability equations in the form of displacement components based on the S-FSDT including the couple stress effect are expressed as follows:

$$\begin{aligned} &H_{44}\frac{\partial^2 w_s}{\partial x^2} + H_{55}\frac{\partial^2 w_s}{\partial y^2} + k_1 N_{xx}\left(\frac{\partial^2 w_b}{\partial x^2}+\frac{\partial^2 w_s}{\partial x^2}\right) + k_2 N_{yy}\left(\frac{\partial^2 w_b}{\partial y^2}+\frac{\partial^2 w_s}{\partial y^2}\right) \\ &-A_s\left[\frac{1}{2}\left(5\frac{\partial^4 w_b}{\partial x^2 \partial y^2}+3\frac{\partial^4 w_s}{\partial x^2 \partial y^2}\right)-\frac{1}{4}\left(\frac{\partial^4 w_b}{\partial x^4}+\frac{1}{2}\frac{\partial^4 w_s}{\partial x^4}+\frac{\partial^4 w_b}{\partial y^4}+\frac{1}{2}\frac{\partial^4 w_s}{\partial y^4}\right)\right]=0 \\ &D_{11}\frac{\partial^4 w_b}{\partial x^4}+\left(2D_{12}+2D_{66}\right)\frac{\partial^4 w_b}{\partial x^2 \partial y^2}+D_{22}\frac{\partial^4 w_b}{\partial y^4}+k_1 N_{xx}\left(\frac{\partial^2 w_b}{\partial x^2}+\frac{\partial^2 w_s}{\partial x^2}\right)+k_2 N_{yy}\left(\frac{\partial^2 w_b}{\partial y^2}+\frac{\partial^2 w_s}{\partial y^2}\right) \\ &-A_s\left[\frac{5}{2}\left(2\frac{\partial^4 w_b}{\partial x^2 \partial y^2}+\frac{\partial^4 w_s}{\partial x^2 \partial y^2}\right)-\frac{1}{4}\left(2\frac{\partial^4 w_b}{\partial x^4}+\frac{\partial^4 w_s}{\partial x^4}+2\frac{\partial^4 w_b}{\partial y^4}+\frac{\partial^4 w_s}{\partial y^4}\right)\right]=0 \end{aligned} \tag{21a-b}$$

3. Exact solution procedure

In this study, different analytical boundary conditions are applied to solve the obtained stability equations which can be written in an explicit mathematically form as [35]

$$\text{Free edge (F):}\quad X_i = \left[\sin^2(\alpha_i x_i)+1\right]\cos^2(\alpha_i x_i)\ ;\ i=1,2 \tag{22a}$$

$$\text{Clamped (C):}\quad X_i = \sin^2(\alpha_i x_i)\ ;\ i=1,2 \tag{22b}$$

$$\text{Simply supported (S):}\quad X_i = \sin(\alpha_i x_i)\ ;\ i=1,2 \tag{22c}$$

where m and n are the half wave numbers, α1=mπ/Lx, α2=nπ/Ly, x1=x, x2=y or terms used in the x and y directions to represent the displacement functions. The displacement function is used in the following form:

$$w_k(x,y) = W_k X_i X_j\ ;\ k=s,b;\ i=1,2\ ;\ j=1,2 \tag{23}$$

By substituting the expression of w_k in Eq. (21), the explicit relation for buckling loads with various boundary conditions can be obtained. The stability equations and closed-form boundary conditions yield a set of algebraic equations as follows:

$$\begin{Bmatrix} Eq.20a \\ Eq.20b \end{Bmatrix} = \begin{bmatrix} k_{11} & k_{12} \\ k_{21} & k_{22} \end{bmatrix} \begin{Bmatrix} W_b \\ W_s \end{Bmatrix} \tag{24}$$

K, I and j (i, j=1, 2) are the coefficients of constant terms for which the following equation is employed to obtain the critical load:

$$q = \begin{bmatrix} Eq.21a & Eq.21b \end{bmatrix},\ u = \begin{bmatrix} W_b & W_s \end{bmatrix} \tag{25}$$

$$J = jacobian(q,u) \rightarrow \det[J] = 0 \tag{26}$$

4. Results and Discussion

The results of the validation and the comparison with other research results should obviously be carried out before investigating various parameters of this study. Therefore, Tables 1 and 2 are examined in order to compare and validate these formulation results with those of other studies. In order for the results to be compared in Tables 1 and 2, [19] and [36] studies are employed while their results were obtained using the first order shear deformation theory, the differential quadrature method (DQM) as well as the Eringen nonlocal elasticity theory. The [37] study is added for further confirmation due to the minor errors in the numerical solutions while its results were obtained through the molecular dynamics solution. Therefore, observing numerical solutions alone does not enable us to ascertain the fact that the present results are validated due to the difference between the results in both cases. However, by examining Tables 1 and 2, one can strongly express that the modified first order shear deformation theory (S-FSDT) results appropriately correspond to the molecular dynamic results. Since this solution is an exact one, this proximity of the results clearly confirms this premise that accurate and appropriate results are obtained by combining the modified first order shear deformation theory and exact solution of the results. Comparing the results shown in Tables 1 with results in Table 2 confirms that the removal of the shear stress correction factors in plates affects the critical load results. Because, when compared with the accurate results, the generated difference in the contractual FSDT by employing this factor is removed in the S-FSDT. According to Tables 1 and 2, the thinner the plate, the closer the results become to the FSDT results and numerical solutions, while their accuracy decreases; because, the FSDT is not applicable in analyzing thin plates and the classical plate theory (CPT) is more applicable in this case. In order to solve stability equations, the parameters in Table 3 which were obtained from related research were employed.

E=1TPa, υ=0.3, h=0.34 nm, μ=1.81nm^2, β=Lx/Ly=1, k1=1, k2=1, k_s=5/6, SSSS [19, 36-37]

E=1TPa, υ=0.3, h=0.34 nm, β=1, k1=1, k2=1, l=2.91nm, η=0, SSSS [Present]

Table 1. Comparison of results of the critical biaxial buckling load for a single-layered graphene sheet and all edges simply supported obtained from the DQ method [19, 36], and the molecular dynamics simulation [37].

Critical buckling load (*Pa.m*)				
Present study	FSDT-DQM [19]	FSDT-DQM [36]	MD results [37]	Lx=Ly (*nm*)
1.0835	1.0749	1.0809	1.0837	4.99
0.6538	0.6523	0.6519	0.6536	8.080
0.4330	0.4356	0.4350	0.4331	10.77
0.2615	0.2645	0.2639	0.2609	14.65
0.1720	0.1751	0.1748	0.1714	18.51
0.1198	0.1239	0.1237	0.1191	22.35
0.0896	0.0917	0.0914	0.0889	26.22
0.0696	0.0707	0.0705	0.0691	30.04
0.0559	0.0561	0.0560	0.0554	33.85
0.0454	0.0453	0.0451	0.0449	37.81

Fig. 2 is presented to show the impact of uniaxial and biaxial loadings. The graphene sheet is determined as square and rectangular in the above-mentioned figure. This investigation is carried out under monotonic and linear loadings due to the changes in *m* and *n* parameters. In the first case, critical load results obtained from *k1=0*, *k2=1* fully corresponds to the results of *k1=1*,*k2=0* (*β=1*); whereas, by investigating the second case and rectangular plates (*β=2)*, it is observed that the results obtained from *k1=1*, *k2*=0 show higher values. Moreover, it is observed that the critical load increases with an increase in m and n values.

Table 2. Comparison of the present results with those of the DQ method [36] and the molecular dynamics (MD) simulation [37] for different aspect ratios of orthotropic single-layered graphene sheets under the uniform biaxial compression.

Critical buckling load (*Pa.m*)			
FSDT-DQM [36]	MD results [37]	S-FSDT, Exact Present study	*Lx/Ly*
0.5115	0.5101	0.5105	0.5
0.5715	0.5693	0.5698	0.75
0.6622	0.6595	0.6599	1.25
0.7773	0.7741	0.7747	1.5
1.0222	1.0183	1.0180	1.75
1.1349	1.1297	1.1301	2

Table 3. Mechanical properties of the nanoplate [22]

Material	Elasticity parameters
nanoplate	$Ex=1765GPa,\ Ey=1588GPa,\ v_{xy}=0.3,\ v_{yx}=Ey\times v_{xy}/Ex,\ h=0.34nm$

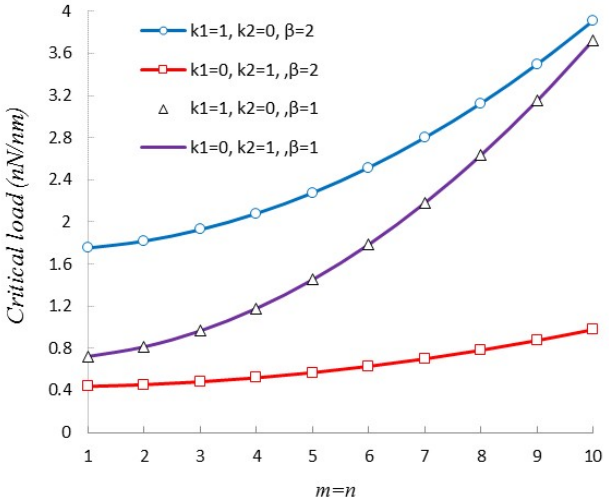

Fig. 2. The effect of the load direction versus wave numbers *(β=Lx/Ly, Ly=10.2nm, l=2h, SSSS, η=1)*

In Fig. 3, the changes of the length scale parameter against different boundary conditions are investigated. As can be seen, critical load results at a variety of boundary conditions increases with an increase in the l parameter as compared with the case in which this impact is disregarded (l=0). According to Fig. 3, the highest critical load is obtained at the CFCF boundary condition and the lowest one is obtained at the SFSF boundary condition. We conclude that the impact of the length scale parameter on the CFCF boundary condition is much higher than its impact on other boundary conditions.

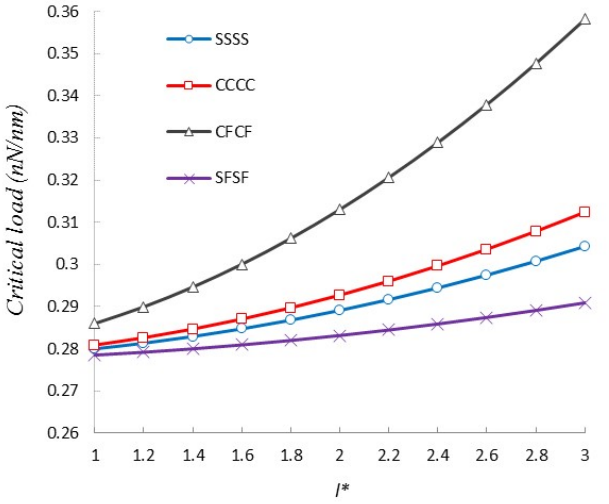

Fig. 3. The length scale parameter versus boundary conditions (η=0.5, k1=k2= 1, l^*=l/h, m=n=1)

In order to determine the impact of the length scale parameter (l) on buckling results, Fig. 4 is provided in which two boundary conditions of CCCC and SSSS with two loading modes are investigated. As the results indicate, the critical load value at CCCC boundary condition is higher than the SSSS value. When disregarding the impact of the length scale, the impact of the loading and boundary condition type is insignificant. In contrast, the increased length parameter results in a higher difference between any loading type in two boundary conditions. This can be inferred from the difference between the results of CCCC, η=0 and SSSS, η=0 at l*>3.

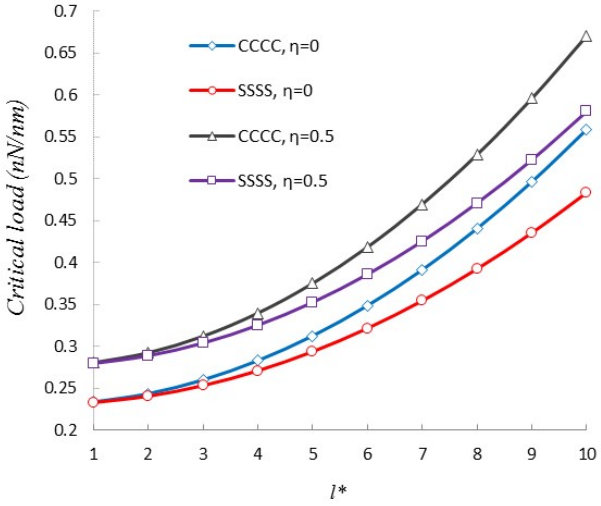

Fig. 4. Variation of the length scale parameter versus the loading type in various boundary conditions (k1=k2=1, l^*=l/h, m=n=1)

The impact of loading types on the nanoplate with the length change of the plate at the CFCF boundary condition was investigated in Fig. 5. As can be seen, within the range of $0<Lx/h<10$, the highest value for the slope of diagram is observed and the highest critical load is obtained. In addition, when loading is considered as a hyperbolic function, the critical load has the lowest value. In fact, in the linear loading, as the in-plane load gets farther from the plate center, the critical load will increase. A possible reason can be the combination of the in-plane torsion to the in-plane pressure. Consequently, as the load center distances from the plate centre in *x* and *y* directions, the pressure decreases and it is substituted by the in-plane torsion while the plate buckles as it twists. Clearly, a higher in-plane torsional force is needed to move the plate into the bucking region.

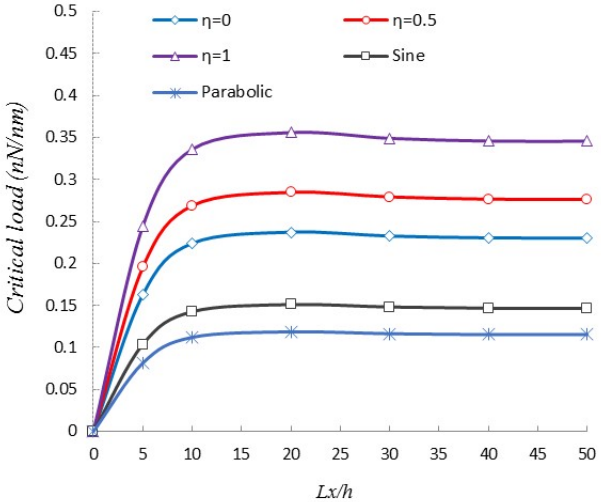

Fig. 5. The effect of various loadings versus the length to the thickness ratio (k1=k2= 1, l=0.5h, m=n=1, CFCF)

5. Conclusion

This study investigated the biaxial non-uniform buckling of a nano graphene sheet. For this purpose, the refined first order shear deformation theory was employed to obtain the governing equations by taking Von-Karman nonlinear strains into account. The size-dependent effect was investigated by using the modified couple stress theory. Moreover, the exact solution was used to extract the results by changing various parameters. In conclusion, some of the important results achieved from the present study are as follows:

* By increasing the parameter β, the impact of uniaxial loads on the results of the critical buckling loads increases.
* The maximum critical load is at the CFCF boundary condition and the minimum is at the SFSF.
* The length scale impact on the results of any boundary conditions increases with an increase in l parameters.

References

[1] de La Fuente, J., "CEO Graphenea" j.delafuente@graphenea.com.
[2] Walker, L.S., Marotto, V.R., Rafiee, M.A., Koretkar, N., Corral, E.L. "Toughening in graphene ceramic composites", ACS Nano. 5, pp. 3182-90, 2011.
[3] Kvetkova, L., Duszova, A., Hvizdos, P., Dusza, J., Kun, P., Balazsi, C. "Fracture toughness and toughening mechanisms in graphene platelet reinforced Si 3 composites", Scripta Materialia. 66, pp. 793-796, 2012.
[4] Liang, J., Huang, Y., Zhang, L., Wang, Y., Ma, Y., Guo, T., Chen, Y. "Molecular-level dispersion of graphene into poly (vinyl alcohol) and effective reinforcement of their nanocomposites", Advanced Functional Materials. 19, pp. 2297-2302, 2009.
[5] Rafiee, M.A., Rafiee, J., Srivastana, I., Wang, Z., Song, H., Yu, Z-Z., Koratkar, "Fracture and fatigue in graphene nanocomposites", Small. 6, pp. 179-83, 2010.
[6] Civalek, O., Demir, Ç. Akgöz, B. "Free Vibration and Bending Analysis of Cantilever Microtubules Based on Nonlocal Continuum Model", Mathematical and Computational Applications. 15, pp. 289-298, 2010.
[7] Akgöz, B., Civalek, o. "Strain gradient elasticity and modified couple stress models for buckling analysis of axially loaded micro-scaled beams", International Journal of Engineering Science. 49, pp. 1268-1280, 2011.
[8] Malekzadeh, P., Setoodeh, A.R., Beni, A.A. "Small scale effect on the thermal buckling of orthotropic arbitrary straight-sided quadrilateral nanoplates embedded in an elastic medium", Composite Structures. 93, pp. 2083-2089, 2011.
[9] Zenkour, A.M., Sobhy, M. "Nonlocal elasticity theory for thermal buckling of nanoplates lying on Winkler–Pasternak elastic substrate medium", Physica E. 53, pp. 251-259, 2013.
[10] Murmu, T., Sienz, J., Adhikari, S., Arnold, C. "Nonlocal buckling of double-nanoplate-systems under biaxial compression", Composites: Part B. 44, pp. 84-94, 2013.
[11] Wang, Y-Z., Cui, H-T., Li, F-M., Kishimoto, K., "Thermal buckling of a nanoplate with small-scale effects", Acta Mechanical. 224, pp. 1299-1307, 2013.
[12] Malekzadeh, P., Alibeygi, A. "Thermal Buckling Analysis of Orthotropic Nanoplates on Nonlinear Elastic Foundation", Encyclopedia of Thermal Stresses, pp. 4862-4872, 2014.
[13] Mohammadi, M., Farajpour, A., Moradi, A., Ghayour, M. "Shear buckling of orthotropic rectangular graphene sheet embedded in an elastic medium in thermal environment", Composites: Part B. 56, pp. 629-637, 2014.
[14] Radic, N., Jeremic, D., Trifkovic, S., Milutinovic, M. "Buckling analysis of double-orthotropic nanoplates embedded in Pasternak elastic medium using nonlocal elasticity theory", Composites: Part B. 61, pp. 162-171, 2014.
[15] Karlicic, D., Adhikari, S., Murmu, T. "Exact closed-form solution for non-local vibration and biaxial buckling of bonded multi-nanoplate system", Composites: Part B. 66, pp. 328-339, 2014.
[16] Anjomshoa, A., Shahidi, A.R., Hassani, B., Jomehzadeh, E. "Finite Element Buckling Analysis of Multi-Layered Graphene Sheets on Elastic Substrate Based on Nonlocal Elasticity Theory", Applied Mathematical Modelling, 38. pp. 1-22, 2014.
[17] Radebe, I.S., Adali, S. "Buckling and sensitivity analysis of nonlocal orthotropic nanoplates with uncertain material properties", Composites: Part B. 56, pp. 840-846, 2014.
[18] Nguyen, T.K., T. P., Nguyen, B.D., Lee, J., "An analytical solution for buckling and vibration analysis of functionally graded sandwich beams using a quasi-3D shear deformation theory", Composite Structures, doi.org/10.1016/j. compstruct.2015. pp. 074, 2015.
[19] Golmakani, M.E., Rezatalab, J. "Non uniform biaxial buckling of orthotropic Nano plates embedded in an elastic medium based on nonlocal Mindlin plate theory", Composite Structures. 119, pp. 238-250, 2015.
[20] Jamali, M., Shojaee, T., Mohammadi, B. "Uniaxial buckling analysis comparison of nanoplate and nanocomposite plate with central square cut out using domain decomposition method", Journal of Applied and Computational Mechanics. 2, pp. 230-242, 2016.
[21] Zarei, M. Sh., Hajmohammad, M. H., Nouri, A. "Dynamic buckling of embedded laminated nanocomposite plates based on sinusoidal shear deformation theory", Journal of Applied and Computational Mechanics. 2, pp. 254-261, 2016.
[22] Malikan, M., Jabbarzadeh, M., Dastjerdi, Sh. "Non-linear Static stability of bi-layer carbon nanosheets resting on an elastic matrix under various types of in-plane shearing loads in thermo-elasticity using nonlocal continuum", Microsystem Technologies, DOI: 10.1007/s00542, pp. 016-3079-9, 2016.
[23] Mindlin, R. D. "Influence of Rotatory Inertia and Shear on Flexural Motions of Isotropic, Elastic Plates", Transaction of the ASME. 73, pp. 31-38, 1951.
[24] Thai, H-T., Choi, D-H. "A simple first-order shear deformation theory for laminated composite plates", Composite Structures. 106, pp. 754-763, 2013.
[25] Mindlin, R. D. "Tiersten HF. Effects of couple-stresses in linear elasticity", Archive for Rational Mechanics and Analysis. 11, pp. 415-48, 1962.
[26] Toupin, R. A., "Elastic materials with couple stresses", Archive for Rational Mechanics and Analysis. 11, pp. 385-414, 1962.
[27] Koiter, W. T., "Couple stresses in the theory of elasticity", I and II. Proc K Ned Akad Wet (B. 67, pp. 17-44, 1964.
[28] Cosserat, E., Cosserat, F., "Theory of deformable bodies", Scientific Library, 6. Paris: A. Herman and Sons, Sorbonne 6, 1909.

[29] Yang, F., Chong, A.C.M., Lam, D.C.C., Tong, P., "Couple stress based strain gradient theory for elasticity", International Journal of Solids and Structures. 39, pp. 2731-43, 2002.
[30] Akgöz, B., Civalek, O., "Free vibration analysis for single-layered graphene sheets in an elastic matrix via modified couple stress theory", Materials and Design. 42, pp. 164-171, 2012.
[31] Thai, H-T., Thuc, P., Nguyen, T-K., Lee, J., "Size-dependent behavior of functionally graded sandwich microbeams based on the modified couple stress theory", Composite Structures. 123, pp. 337-349, 2015.
[32] Dey, T., Ramachandra, L.S., "Buckling and postbuckling response of sandwich panels under non-uniform mechanical edge loadings", Composites: Part B. 60, pp. 537-545, 2014.
[33] Leissa, A.W., Kang, Jae-Hoon, "Exact solutions for vibration and buckling of an SS-C-SS-C rectangular plate loaded by linearly varying in-plane stresses", International Journal of Mechanical Sciences. 44, pp. 1925-1945, 2002.
[34] Hwang, I., Seh Lee, J., "Buckling of Orthotropic Plates under Various Inplane Loads", KSCE Journal of Civil Engineering. 10, pp. 349–356, 2006.
[35] Malikan, M. "Electro-mechanical shear buckling of piezoelectric nanoplate using modified couple stress theory based on simplified first order shear deformation theory", Applied Mathematical Modelling. 48, pp. 196-207, 2017.
[36] Golmakani, M.E., Sadraee Far, M.N. "Buckling analysis of biaxially compressed double layered graphene sheets with various boundary conditions based on nonlocal elasticity theory", Microsystem Technologies, DOI 10.1007/s00 .pp,542-016-3053-6, 2016.
[37] Ansari, R., Sahmani, S. "Prediction of biaxial buckling behavior of single-layered graphene sheets based on nonlocal plate models and molecular dynamics simulations", Applied Mathematical Modeling. 37, pp. 7338–7351, 2013.